VIP Sensors Very Important Paper

International Edition: DOI: 10.1002/anie.201601346
German Edition: DOI: 10.1002/ange.201601346

A Fluorescent Sensor for Dual-Channel Discrimination between Phosgene and a Nerve-Gas Mimic

Xin Zhou, Yiying Zeng, Chen Liyan, Xue Wu, and Juyoung Yoon**

Abstract: *The ability to analyze highly toxic chemical warfare agents (CWAs) and related chemicals in a rapid and precise manner is essential in order to alleviate serious threats to humankind and public security caused by unexpected terrorist attacks and industrial accidents. In this investigation, we designed a o-phenylenediamine-pyronin linked dye that is capable of both fluorogenic and colorimetric discrimination between phosgene and the prototypical nerve-agent mimic, diethyl chlorophosphate (DCP) in the solution or gas phase. Moreover, this dye has been used to construct a portable kit that can be employed for real-time monitoring of DCP and phosgene in the field, both in a discriminatory manner, and in a simple and safe way.*

Phosgene is a colorless and highly toxic gas. As one of the most toxic substances (among the top 10%), this substance has gained infamy as a chemical weapon agent (CWA) during the World Wars.[1] Exposure to phosgene has severe acute respiratory effects, including noncardiogenic pulmonary edema, pulmonary emphysema, and death.[2] Notably, unlike other deadly CWAs, phosgene has a unique toxicological concerns owing to the existence of an unpredictable asymptomatic latent phase that takes place prior to the onset of life-threatening pulmonary edema.[3] In addition, comparing with other nerve gas agents, such as sarin, soman, and tabun, whose production is strictly controlled and prohibited by laws,[4] phosgene is a widely used industrial starting material.[5] As a consequence, phosgene does pose a serious threat to public health safety, not only because of its potential use by terrorists, but also because of its unexpected release during industrial accidents. Therefore, a strong need exists to develop methods for rapid and accurate detection of phosgene in a manner that enables distinction between this agent and other CWAs.

Recently, methods for the detection of CWAs that utilize fluorescent and colorimetric sensors have attracted attention.[6] The goals of these efforts have been to enhance advantageous features of the sensors, including sensitivity, selectivity, and rapid response time, over those associated with costly conventional procedures.[7] However, in contrast to numerous studies that have focused on the development of fluorescent sensors for nerve-gas agents,[8] only a few have been targeted at the construction of those for phosgene detection.[9] Moreover, to the best of our knowledge, no fluorescent sensor has been described to date that is capable of discriminating between phosgene and other chemical warfare agents by utilizing different emission channels.

As shown in Scheme 1b, existing fluorescent sensors for phosgene/nerve-gas-agent recognition are based on their nucleophilic substitution reactions (phosphorylations or acylations) with alcohol hydroxyl and amine groups in sensors. These transformations lead to suppression of photoinduced electron transfer (PET) quenching of a fluorophore and promote generation of detectable fluorescent signals (or

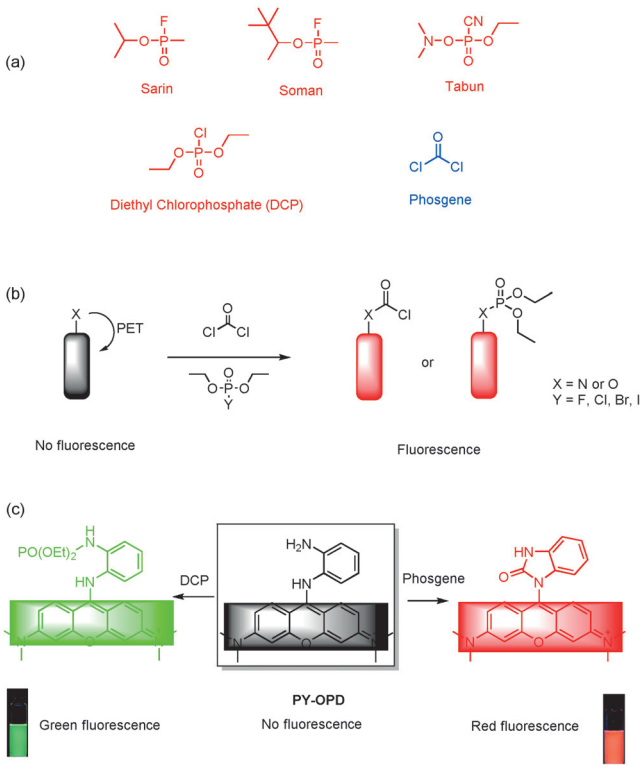

Scheme 1. a) Chemical structures of typical nerve-gas agents sarin, aoman, and tabun, and their mimic diethyl chlorophosphate (DCP), as well as phosgene. Schematic representation of proposed mechanisms responsible for detecting nerve-gas agents and phosgene: b) common strategy based on suppression of PET quenching and resulting recovery of fluorescence. c) The new approach of this work for discriminating between phosgene and DCP.

[*] Dr. X. Zhou, C. Liyan, Prof. J. Yoon
Department of Chemistry and Nano Science
Ewha Womans University
Seoul 120-750 (Korea)
E-mail: jyoon@ewha.ac.kr
Dr. X. Zhou, Y. Zeng, Prof. X. Wu
Key Laboratory of Natural Resources of Changbai Mountain & Functional Molecules, Ministry of Education, Yanbian University
Yanji 133-002 (China)
E-mail: wuxue@ybu.edu.cn

Supporting information for this article can be found under: http://dx.doi.org/10.1002/anie.201601346.

absorption/color signals). Because their nucleophilic substitution reactivities are quite similar, phosgene and nerve-gas agents cannot be effectively distinguished by employing fluorescent sensors that are designed using this strategy.

To this end, in the study described below, we pursued a new rational strategy. The new approach utilizes an interesting phosgene-specific cyclization reaction of a sensor that contains an *o*-phenylenediamine (OPD).[10] In the newly designed sensor (Scheme 1c), this reaction alters the degree of conjugation with a fluorophore, which brings about a change of fluorescence emission. In contrast, we envisioned that other types of nerve-gas agents would promote a different fluorescence response because they are incapable of participation in the same type of cyclization reaction that phosgene undergoes.

This strategy has been successfully tested through studies with the sensor PY-OPD. This sensor, which is not fluorescent as a result of PET-promoted quenching of the fluorescence by the OPD moiety, displays red emission in the presence of phosgene and green emission when the nerve-gas mimic diethyl chlorophosphate (DCP) is present.

We devised a simple, efficient, and safe method to synthesize *meso*-substituted pyronins (Scheme 2). Conventional methods typically involve five steps, require more than five days, and deliver target substances in low overall total yields (< 15 %).[11] Moreover, the highly toxic reactant KCN is required to generate the key synthetic intermediate PY-O.[12] These disadvantages have hampered the preparation and studies of these types of pyronin dyes. In our approach, commercially available pyronin Y dye is directly treated with the sterically hindered base *t*BuOK and elemental sulfur (S_8) under anhydrous condition to produce the corresponding thioketone PY-S in a carbene-based pathway.[13] Because the triflate salt, generated by reaction of PY-S with Tf_2O is highly reactive, its substitution reactions with nucleophiles take place more efficiently than those with the triflate analogue arising from PY-O. Compared to those described previously, the route we developed requires only three steps and far shorter reaction times, and it affords the products in higher yields and also avoids the use of KCN. By using this strategy, we prepared the sensors PY-OPD and its analogues PY-PA, and PY-PPD employed in model studies.

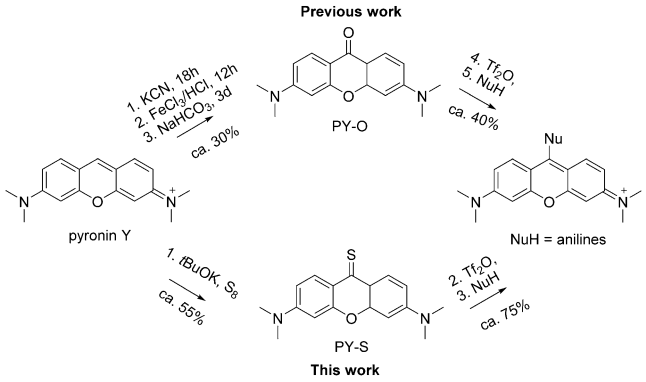

Scheme 2. Synthetic routes to *meso*-aniline-substituted pyronin dyes. Previous routes and the proposed new strategy.

The fluorescence response of PY-OPD towards phosgene was investigated first. In order to avoid handling volatile phosgene during titration experiments, its nonvolatile and less toxic counterpart triphosgene was used. This substance is a well-known precursor that generates phosgene in situ. The spectra in Figure 1a show that PY-OPD is almost nonfluorescent ($\Phi_F = 0.0003$ with rhodamine B as the reference) owing to the well-demonstrated quenching of its singlet excited state by PET from the OPD moiety to the pyronin fluorophore. Upon addition of triphosgene, a new emission peak centered at 593 nm grows to an intensity that is 580 times larger than that of the original solution. This phenomenon is accompanied by the observed formation of red fluorescence (Figure 1a inset), which is easily visualized by using a hand-held UV lamp (365 nm). Notably, the changes that PY-OPD undergoes upon addition of triphosgene take place rapidly so that the overall sensing process is accomplished within 2 min (Figure S1 in the Supporting Information). Moreover, the sensing process can be finished within several seconds if trimethylamine is present in the assay mixture to promote rapid formation of phosgene. Inspection of a fit of the titration data (Figure S2), shows that PY-OPD has a low triphosgene detection limit of 20 nM. To the best of our knowledge, the new sensor is more sensitive to this toxic substance than others described previously. In addition to the

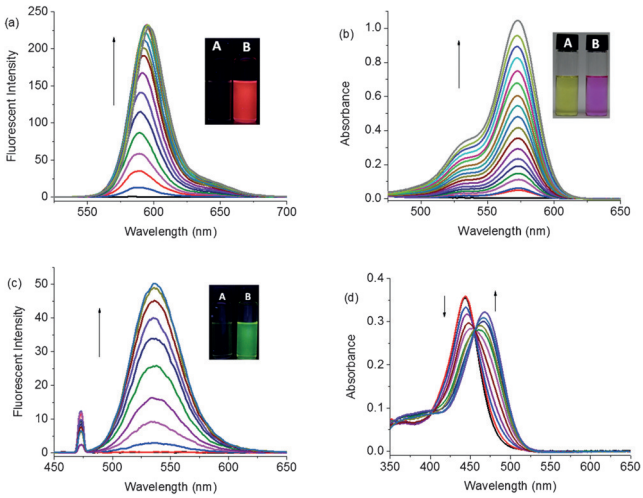

Figure 1. Fluorescence (a) and absorbance (b) spectra of PY-OPD in chloroform (10 μM) upon gradual addition of a solution of triphosgene (0–2 equiv) in chloroform ($\lambda_{ex} = 580$ nm, slits: 1.5 nm). Each spectrum was recorded after 2 min. Inset: colorimetric and fluorescent responses of PY-OPD towards phosgene, (A) represents free PY-OPD, (B) represents PY-OPD-phosgene adduct. Fluorescence (c) and absorbance (d) spectra of a chloroform solution of PY-OPD (10 μM) upon gradual addition of a chloroform solution of DCP (0–100 equiv) ($\lambda_{ex} = 470$ nm, slits: 1.5 nm). Each spectrum was recorded over 2 min. Inset: fluorescence responses of PY-OPD towards DCP, (A) represents free PY-OPD, (B) represents PY-OPD-DCP adduct. Fluorescence images were obtained under irradiation with a 365 nm ultraviolet lamp.

dramatic fluorescence response, PY-OPD undergoes a naked-eye-observable color change upon addition of triphosgene (see Figure 1 b). Specifically, a new visible-absorption peak at 580 nm (violet) arises when the toxic agent is added to a yellow solution of the sensor (Figure 1 b inset). Notably, PY-OPD showed high selectivity towards phosgene, other mimics (including chlorides and chloroacetyl chloride) do not display the same fluorescence responses (Figure S10).

Next, the responses of PY-OPD elicited by the nerve-agent mimic DCP was probed by using fluorescence and UV/Vis spectroscopy. The emission spectra displayed in Figure 1 c show that, unlike the response to phosgene in which red florescent emission emerges, addition of DCP to a chloroform solution of PY-OPD causes a gradual growth of a new and more intense peak at 538 nm corresponding to green fluorescent emission (Figure 1 c inset). In addition, the intensity of the 444 nm absorption band of PY-OPD gradually decreases, and is replaced by a new peak at 468 nm with an observable isosbestic point at 455 nm. It is notable that addition of DCP to PY-OPD does not promote formation of an emission peak around 600 nm and or an absorbance peak around 580 nm, both of which are observed when triphosgene is added to this sensor.

As mentioned above, PY-OPD responds in a discriminatory manner when subjected to phosgene and DCP. Based on the observations made, we are able to propose the plausible mechanism (Scheme 3) for the reaction of PY-OPD with phosgene to result in benzimidazolone product **P1**. In this transformation, the electron-donating amine groups in PY-OPD are converted to an electron-withdrawing urea group. As stated above, this process results in blocking PET fluorescent quenching and also altering the HOMO–LUMO energy gap of the fluorophore, thus resulting in strong red emission and the naked-eye-observable color change.

To gain evidence to support this mechanistic proposal, ESI-MS and NMR spectroscopy were utilized to detect the product **P1** that results from mixing PY-OPD with phosgene. Analysis of mass spectrometric data (Figure S3 and S4) showed that the peak at m/z 373.3 corresponding to the molecular ion of PY-OPD disappears following addition of phosgene, and a new peak grows at m/z 399.2 corresponding to **P1**. Notably, no peaks other than those associated with these two substances are present in the MS spectra recorded during the course of this analysis, thus indicating the formation of **P1** from PY-OPD is quantitative. Formation of **P1** was also confirmed by carrying out ^{1}H NMR titration experiments. Inspection of the spectra (Figure S5), recorded after adding phosgene to a solution of PY-OPD, shows that some of the resonances for the protons in the OPD moiety shift to lower fields, thus indicating the formation of **P1**. Finally, **P1** was isolated from the reaction mixture and characterized by using ^{1}H and ^{13}C NMR spectroscopy (see the Supporting Information).

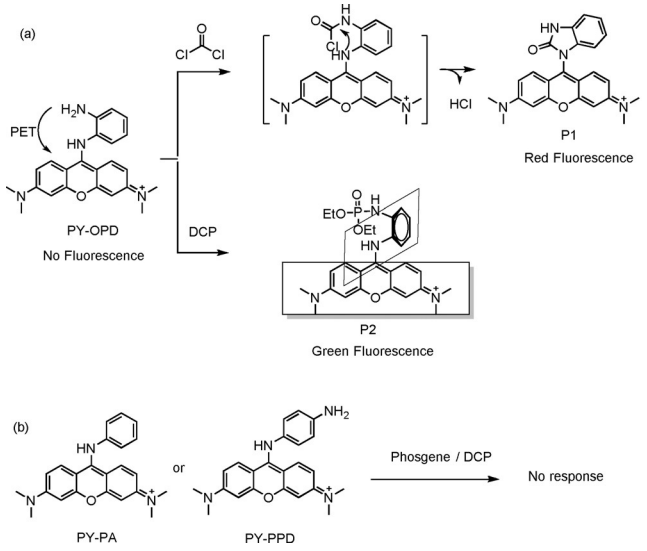

Scheme 3. a) Proposed mechanism for chemical reactions that lead to discriminative sensing by PY-OPD for phosgene and DCP. b) Structure of sensors PY-PA and PY-PPD used for control studies.

In contrast, PY-OPD reacts with DCP to produce **P2**, in which only the more reactive primary NH_2 group is phosphorylated. This conversion causes a change in the fluorescence signal as a result of partially blocking the PET quenching effect. Unfortunately, we were unable to perform MS spectrometric analysis of **P2** owing to the fact that loss of the phosphate ester group takes place too rapidly to allow detection of the molecular ion.[14] As a result, we employed acetyl chloride (AC) to mimic the potential reactivity of PY-OPD with an electrophile capable of undergoing only a single acylation reaction and not ensuing cyclization. The adduct produced by reaction of the sensor with AC has similar emission and absorption characteristic (Figure S6) as the one generated by reaction between the sensor and DCP. Moreover, analysis of ESI-MS data of the product (molecular ion at m/z 415.3; Figure S7) showed that, as expected, it is a mono-acetamide derivative.

PY-PA and PY-PPD were prepared and employed as controls. These substances are incapable of reacting with phosgene to produce benzimidazolone derivatives in secondary cyclization processes. Interestingly, PY-PA and PY-PPD are initially nonfluorescent, and addition of phosgene or DCP to a solution of either PY-PA or PY-PPD does not bring about an emission or colorimetric response (Figure S8 and S9). The observation made with PY-PPD is a little surprising because this model contains a primary *para*-amine group, which should be a reactive nucleophile. A plausible reason may be the different molecular configuration of their DCP adducts. As showed in Scheme 3 a, in the case of the adduct **P2**, the dihedral angle between the PET donor moiety (OPD) and the xanthene ring is almost vertical because of the large steric hindrance effect of phosphoramide group, which suppressed the PET effect more efficiently, thus resulting in the restoration of the fluorescence.[15] In contrast, the adduct PY-PPD-DCP may adopt a more planar configuration, in which the PET effect is still sufficiently robust to quench the fluorescence.

The highly desirable features of PY-OPD were used advantageously in the fabrication of a practical sensor for the detection of phosgene and DCP. For this purpose, PY-OPD was immobilized on a polyethylene oxide membrane (Figure S11). The membrane, which contains only a small amount

of the sensor, is initially transparent and colorless, and it emits a weak blue fluorescence under a hand-held UV lamp (365 nm). After exposure of the membrane to various amounts of phosgene vapor (0–20 ppm) for several seconds, the color of its fluorescent signal becomes pink-red (Figure 2a). Also, the color of the membrane changes from

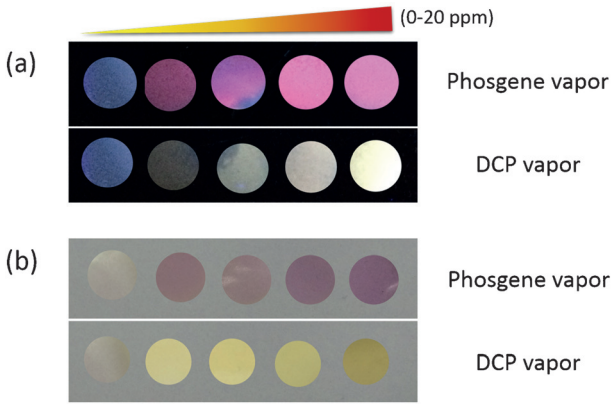

Figure 2. Fluorescence (a) and color (b) responses of PY-OPD based polyethylene oxide membrane upon exposure to various amounts of phosgene and DCP vapor (0–20 ppm), respectively.

colorless to violet (Figure 2b), which can be readily detected by using the naked eye. In contrast, exposure of the membrane to DCP vapor promotes a change in the color of the fluorescence signal to pale white, along with a color change from colorless to yellow. These observations indicate that the strategy we devised has led to the development of a safe and simple method for rapid discriminatory sensing of trace amounts of phosgene and DCP.

In summary, we have developed the first reported fluorescent and colorimetric sensor for selective detection of phosgene and the nerve-agent mimic DCP. The sensor PY-OPD is readily synthesized by using a modified carbene-type reaction. Owing to the uniquely different reactivities of this sensor with phosgene and DCP, distinctly different color and emission responses are observed. Finally, a practical sensor for phosgene and the nerve-agent mimic was fabricated by immobilizing PY-OPD on a polymer membrane. The new chemically based strategy has led to the design and production of a safe and simple method for quickly detecting of quantities of CWAs that are at or below concentration levels that pose a health risk.

Acknowledgements

This work was supported by a grant from the National Creative Research Initiative programs of the National Research Foundation of Korea (NRF) funded by the Korean government (MSIP; No. 2012R1A3A2048814). X. Zhou thanks to the Youth Science Foundation of Jilin Province (20160520003JH).

Keywords: carbenes · fluorescence · nerve-gas mimics · phosgene · sensors

How to cite: *Angew. Chem. Int. Ed.* **2016**, *55*, 4729–4733
Angew. Chem. **2016**, *128*, 4807–4811

[1] a) J. Borak, W. F. Diller, *J. Occup. Environ. Med.* **2001**, *43*, 110–119; b) D. Evison, D. Hinsley, P. Rice, *Br. Med. J.* **2002**, *324*, 332–335; c) C. B. Bast, D. F. Glass-Mattie in *Handbook of Toxicology of Chemical Warfare Agents*, 2nd ed. (Ed.: R. C. Gupta), Academic Press, Boston, **2015**, pp. 327–335.

[2] a) R. G. Danzinger, A. F. Hofmann, L. J. Schoenfield, J. L. Thistle, *N. Engl. J. Med.* **1972**, *286*, 1–8; b) D. E. Rowe, R. J. Carroll, C. L. Day, *J. Am. Acad. Dermatol.* **1992**, *26*, 976–990; c) E. D. Robin, C. E. Cross, R. Zelis, *N. Engl. J. Med.* **1973**, *288*, 292–304; d) N. C. Staub, *Physiol. Rev.* **1974**, *54*, 678–811.

[3] S. C. Gad in *Encyclopedia of Toxicology*, 3rd ed. (Ed.: P. Wexler), Academic Press, Oxford, **2014**, pp. 904–906.

[4] a) R. Price, *International Organization* **1995**, *49*, 73–103; b) A. Watson, D. Opresko, R. A. Young, V. Hauschild, J. King, K. Bakshi in *Handbook of Toxicology of Chemical Warfare Agents*, 2nd ed. (Ed.: R. C. Gupta), Academic Press, Boston, **2015**, pp. 87–109.

[5] *Topics in Inorganic and General Chemistry, Vol. 24* (Eds.: T. A. Ryan, E. A. Seddon, K. R. Seddon), Elsevier, **1996**, pp. 167–221.

[6] a) S.-W. Zhang, T. M. Swager, *J. Am. Chem. Soc.* **2003**, *125*, 3420–3421; b) T. J. Dale, J. Rebek, *J. Am. Chem. Soc.* **2006**, *128*, 4500–4501; c) M. Burnworth, S. J. Rowan, C. Weder, *Chem. Eur. J.* **2007**, *13*, 7828–7836; d) H. J. Kim, J. H. Lee, H. Lee, J. H. Lee, J. H. Lee, J. H. Jung, J. S. Kim, *Adv. Funct. Mater.* **2011**, *21*, 4035–4040; e) A. M. Costero, M. Parra, S. Gil, R. Gotor, R. Martínez-Mañez, F. Sancenón, S. Royo, *Eur. J. Org. Chem.* **2012**, *2012*, 4937–4946; f) A. Barba-Bon, A. M. Costero, S. Gil, A. Harriman, F. Sancenon, *Chem. Eur. J.* **2014**, *20*, 6339–6347; g) S. Royo, A. M. Costero, M. Parra, S. Gil, R. Martinez-Manez, F. Sancenon, *Chem. Eur. J.* **2011**, *17*, 6931–6934.

[7] a) Y. C. Yang, J. A. Baker, J. R. Ward, *Chem. Rev.* **1992**, *92*, 1729–1743; b) S. L. Bartelt-Hunt, D. R. U. Knappe, M. A. Barlaz, *Crit. Rev. Environ. Sci. Technol.* **2008**, *38*, 112–136; c) M. Palit, D. Pardasani, A. K. Gupta, D. K. Dubey, *Anal. Chem.* **2005**, *77*, 711–717; d) M. A. Mäkinen, O. A. Anttalainen, M. E. T. Sillanpää, *Anal. Chem.* **2010**, *82*, 9594–9600.

[8] a) Z. Lei, Y. Yang, *J. Am. Chem. Soc.* **2014**, *136*, 6594–6597; b) B. Diaz de Greñu, D. Moreno, T. Torroba, A. Berg, J. Gunnars, T. Nilsson, R. Nyman, M. Persson, J. Pettersson, I. Eklind, P. Wasterby, *J. Am. Chem. Soc.* **2014**, *136*, 4125–4128; c) V. Kumar, E. V. Anslyn, *J. Am. Chem. Soc.* **2013**, *135*, 6338–6344; d) A. Barba-Bon, A. M. Costero, S. Gil, R. Martinez-Manez, F. Sancenon, *Org. Biomol. Chem.* **2014**, *12*, 8745–8751; e) R. Gotor, A. M. Costero, P. Gaviña, S. Gil, *Dyes Pigm.* **2014**, *108*, 76–83; f) S. Royo, R. Martínez-Máñez, F. Sancenón, A. M. Costero, M. Parra, S. Gil, *Chem. Commun.* **2007**, 4839; g) S. Goswami, A. Manna, S. Paul, *RSC Adv.* **2014**, *4*, 21984; h) S. Sarkar, R. Shunmugam, *Chem. Commun.* **2014**, *50*, 8511–8513; i) S. Sarkar, A. Mondal, A. K. Tiwari, R. Shunmugam, *Chem. Commun.* **2012**, *48*, 4223–4225; j) W. Xuan, Y. Cao, J. Zhou, W. Wang, *Chem. Commun.* **2013**, *49*, 10474–10476; k) Y. J. Jang, D. P. Murale, D. G. Churchill, *Analyst* **2014**, *139*, 1614–1617; l) J. R. Hiscock, F. Piana, M. R. Sambrook, N. J. Wells, A. J. Clark, J. C. Vincent, N. Busschaert, R. C. Brown, P. A. Gale, *Chem. Commun.* **2013**, *49*, 9119–9121.

[9] a) H. Zhang, D. M. Rudkevich, *Chem. Commun.* **2007**, 1238–1239; b) X. Wu, Z. Wu, Y. Yang, S. Han, *Chem. Commun.* **2012**, *48*, 1895–1897; c) P. Kundu, K. C. Hwang, *Anal. Chem.* **2012**, *84*, 4594–4597.

[10] a) R. L. Clark, A. A. Pessolano, *J. Am. Chem. Soc.* **1958**, *80*, 1657–1662; b) R. Henning, R. Lattrell, H. J. Gerhards, M. Leven, *J. Med. Chem.* **1987**, *30*, 814–819.

[11] a) L. Wu, K. Burgess, *Org. Lett.* **2008**, *10*, 1779–1782; b) T. Pastierik, P. Sebej, J. Medalova, P. Stacko, P. Klan, *J. Org. Chem.*

2014, *79*, 3374 – 3382; c) J. Liu, Y.-Q. Sun, H. Zhang, Y. Huo, Y. Shi, W. Guo, *Chem. Sci.* **2014**, *5*, 3183; d) H. Zhang, J. Liu, Y. Q. Sun, Y. Huo, Y. Li, W. Liu, X. Wu, N. Zhu, Y. Shi, W. Guo, *Chem. Commun.* **2015**, *51*, 2721 – 2724; e) Y. Q. Sun, J. Liu, H. Zhang, Y. Huo, X. Lv, Y. Shi, W. Guo, *J. Am. Chem. Soc.* **2014**, *136*, 12520 – 12523.

[12] S. Kenmoku, Y. Urano, H. Kojima, T. Nagano, *J. Am. Chem. Soc.* **2007**, *129*, 7313 – 7318.

[13] a) S. Sugawara, S. Kojima, Y. Yamamoto, *Chem. Commun.* **2012**, *48*, 9735 – 9737; b) S. Gómez-Bujedo, M. Alcarazo, C. Pichon, E. Alvarez, R. Fernandez, J. M. Lassaletta, *Chem. Commun.* **2007**, 1180 – 1182.

[14] a) J. DeGnore, J. Qin, *J. Am. Soc. Mass Spectrom.* **1998**, *9*, 1175 – 1188; b) G. E. Reid, R. J. Simpson, R. A. J. O'Hair, *J. Am. Soc. Mass Spectrom.* **2000**, *11*, 1047 – 1060; c) S. D. Richardson, *Chem. Rev.* **2001**, *101*, 211 – 254.

[15] a) H. Kobayashi, M. Ogawa, R. Alford, P. L. Choyke, Y. Urano, *Chem. Rev.* **2010**, *110*, 2620 – 2640; b) T. Miura, Y. Urano, K. Tanaka, T. Nagano, K. Ohkubo, S. Fukuzumi, *J. Am. Chem. Soc.* **2003**, *125*, 8666 – 8671.

Received: February 5, 2016
Published online: March 3, 2016

